A PARALLEL IMPLEMENTATION OF UNSTEADY SIMULATION OF DOWNSTREAM WAKE GENERATED BY A FLAPPING FLAT PLATE

Abhijeet R. Nair
AE20B101
Department of Aerospace Engineering
Indian Institute of Technology Madras
Chennai - 600036
Email: ae20b101@smail.iitm.ac.in

ABSTRACT

Aerodynamics research often draws inspiration from nature, and biomimetic flows are crucial. For instance, analyzing the aerodynamics of flapping bird wings provides valuable insights. Unlike conventional fixed-wing aircraft, birds' flapping wings demonstrate remarkable energy efficiency, especially at their characteristic scale and speed. Leveraging this natural phenomenon, engineers aspire to design aerial vehicles that use flapping wings called ornithopters. This is especially useful for the scale of micro UAVs.

A detailed understanding of the aerodynamics associated with flapping motion is essential to achieve this goal. One critical aspect is capturing the downstream wake generated during motion and assessing its impact on wing load generation. In this context, the presented project simulates the unsteady wake downstream of a vertically oscillating flat plate in a freestream.

The code is parallelized using OpenMP. The performance of the serial and parallel codes is also compared through metrics.

NOMENCLATURE

ϕ Velocity potential
$\boldsymbol{v}$ Velocity vector
Γ Circulation
U_∞ Freestream velocity
α Angle of attack

INTRODUCTION

This project considers a flat plate oscillating vertically according to a sinusoidal motion kept in a freestream at a certain angle of attack. For a numerical simulation, the body will be discretized into several collocation points, each being the location of a vortex (called the body vortices). At each time step, the motion of the wake vortices will be determined. The effect of these vortices on the force felt by the flat plate will be computed. The theory behind the simulation is also explained in this report.

THEORY

Potential Flow Theory:

The potential flow is described as irrotational, i.e., it has no vorticity. Along with the incompressibility condition, the following can be derived from the continuity equation:

$$\nabla^2\phi = 0 \tag{1}$$

which is the Laplace equation. The solution to this equation depends on the different boundary conditions arising from the problem. The most important boundary used is the condition of the zero normal flow. It that the normal component of the relative velocity between the fluid and the solid surface (like that of a body) is zero on the boundary:

$$\boldsymbol{v}\cdot\boldsymbol{n} = 0 \tag{2}$$

where, $\boldsymbol{n}$ is the normal vector of the surface.

It must be noted that the Laplace equation is a linear homogeneous differential equation. Thus, a linear combination is also a solution given any two solutions. This superposition property

is used to superimpose certain elementary flows (like sources, sinks, and point vortex) to generate flow over any body. For a lifting flow around any body (like an airfoil), we need to have a point vortex.

Kelvin's Circulation Theorem:

Another property of an inviscid incompressible flow is the Kelvin's Circulation Theorem. This is stated as [1]:

> The time rate of change of circulation around a closed curve consisting of the same fluid elements is zero.

Here, circulation is a measure of the fluid rotation over a finite region. It is defined as:

$$\Gamma = \oint_C \boldsymbol{v} \cdot \boldsymbol{dl} \tag{3}$$

where C is the contour around which the circulation is calculated. Thus, Kelvin's Theorem is written as:

$$\frac{D\Gamma}{Dt} = 0 \tag{4}$$

An application of this theorem is in the following situation. Consider an airfoil with zero velocity. Thus, there is no circulation around it. Now, if it is suddenly set into motion, the body vortex will have a circulation. Thus, considering a contour containing identical fluid particles before and after the start of motion, the rate of change of Γ is non-zero. This violates Kelvin's Theorem. Thus, to compensate for this, a vortex is generated by the airfoil at the trailing edge, called the wake vortex, which has the same strength as the body vortex. This is seen in Fig. 1.

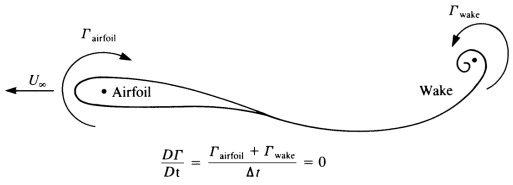

FIGURE 1. Wake generated by an airfoil [1]

Point Vortex:

As mentioned before, one of the elementary solutions of the Laplace equation is the point vortex. This leads to a velocity with no radial velocity, i.e.,

$$\begin{aligned} v_r &= 0 \\ v_\theta &= v_\theta(r, \theta) \end{aligned} \tag{5}$$

When this form is substituted in the continuity equation in cylindrical coordinates, it turns out that v_θ is a function of radial distance from the vortex only, i.e., $v_\theta = v_\theta(r)$. From the irrotational property, it can be shown that:

$$v_\theta = \frac{k}{r} \tag{6}$$

where k is a constant. If the vortex has a circulation of Γ:

$$k = -\frac{\Gamma}{2\pi} \tag{7}$$

Thus, the velocity field is:

$$\begin{aligned} v_r &= 0 \\ v_\theta &= -\frac{\Gamma}{2\pi r} \end{aligned} \tag{8}$$

The velocity potential of the vortex is given as:

$$\phi = -\frac{\Gamma}{2\pi}\theta \tag{9}$$

It can be shown that this function indeed satisfies the Laplace equation. The velocity potential and the field in Cartesian coordinates are given as:

$$\begin{aligned} \phi &= -\frac{\Gamma}{2\pi}\tan^{-1}\frac{y-y_0}{x-x_0} \\ u &= \frac{\Gamma}{2\pi}\frac{y-y_0}{(x-x_0)^2+(y-y_0)^2} \\ v &= -\frac{\Gamma}{2\pi}\frac{x-x_0}{(x-x_0)^2+(y-y_0)^2} \end{aligned} \tag{10}$$

Lumped Vortex Model:

According to the thin airfoil theory (TAT), the lifting behaviour of an airfoil is explained by approximating the airfoil as a vortex sheet, as shown in Fig. 2.

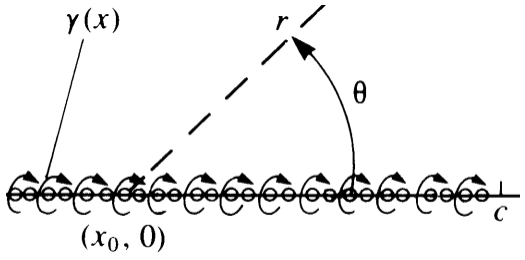

FIGURE 2. Vortex sheet model for a thin airfoil [1]

This model can be simplified further by discretizing the entire airfoil into a set of panels, each containing a single *lumped vortex*, which has the circulation equivalent to the entire panel. The vortex is placed at the quarter chord of the panel since the centre of pressure is located there. Also, the zero normal flow boundary, specified over the entire plate in TAT, is again specified at one point in the entire panel. It can be shown that, to produce the same results as TAT, this *collocation point* should be at the three-quarter chord of the panel. This is shown in Fig. 3. The same lumped vortex model will be used for the unsteady flapping simulation.

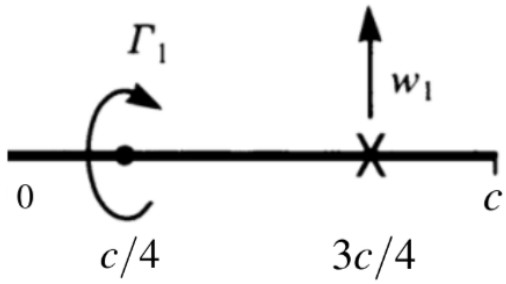

FIGURE 3. Lumped vortex model of an airfoil [1]

Influence Coefficients:
For a given panel, with its vortex located at (x_0, y_0) according to a Cartesian coordinate system, the *induced* velocity of the flow at any point (x, y) can be calculated using the last equations of Eqn. 10. Now, since an airfoil is discretized into a set of panels, their relative location is always constant. Thus, if a body-fixed coordinate system is considered, the induced velocity can be calculated at each collocation point due to a vortex, considering a unit circulation for the vortex. Then, once the vortex strength is computed, the velocity can be scaled by the value to get the correct value.

Since the interest is in enforcing a no-normal flow condition, only the v-component of the induced velocity is needed. Thus, all these v-components called *influence coefficients*, can be computed and collected into a matrix A. Thus:

$$\begin{aligned} A &= [A_{ij}] \\ &= v(1, x_{ci}, y_{ci}, x_{vj}, y_{vj}) \\ &= -\frac{1}{2\pi} \frac{x_{ci} - x_{vj}}{(x_{ci} - x_{vj})^2 + (y_{ci} - y_{vj})^2} \end{aligned} \tag{11}$$

where, x_{ci} is the x-coordinate of the collocation point of i-th panel and x_{vj} is the x-coordinate of the vortex of j-th panel, and so on. Thus, A will be a square matrix of size $N \times N$, where N is the number of panels.

Now, at each time step, a new wake vortex is released (*shed*) into the flow by the airfoil. Thus, at the m-th time step, there will be m wakes. The idea of influence coefficients can be extended to the wakes as well. Thus, define the matrix B as:

$$\begin{aligned} B &= [B_{ij}] \\ &= v(1, x_{ci}, y_{ci}, x_{wj}, y_{wj}) \end{aligned} \tag{12}$$

However, note that the wakes are free to move here relative to the airfoil. Thus, the locations of wakes $1, ..., m-1$ cannot be known beforehand; it has to be computed at each time step. So, the elements of B corresponding to them must be updated at each time step. The new wake is released at a fixed initial location, which will be updated once the induced velocities due to other vortices are calculated. This location needs to be quite close to the trailing edge. Thus, let it be $0.1dx$ after the trailing edge, where dx is the length of each panel. Thus, the elements of Bim, $i = 1, ..., N$ are fixed for all time steps.

The B matrix is thus a vector of size $N \times m$ at time step m. Both these matrices are called the influence coefficient matrices. The algorithm will be described in the next section.

WAKE CAPTURE ALGORITHM

In this implementation, a flat plate is considered to be flapping in a free stream (with velocity U_∞) at an angle of attack α. There are two frames of reference here. One is the fluid-fixed frame. In this frame, the body will appear moving forward with an up-down motion. This will be used as default locations and velocities. The second frame is the body-fixed frame, which is used more easily to write the boundary condition equations. Thus, at a time instant t, the origin of the plate will be located at $(x_0(t), y_0(t))$, moving with a velocity of $(U_\infty, \dot{y}(t))$. The collocation and vortex locations will be computed with respect to the origin. The location of the new wake will be:

$$\begin{aligned} x_w(t) &= x_0(t) + (c + 0.1dx)\cos\alpha \\ y_w(t) &= y_0(t) - (c + 0.1dx)\sin\alpha \end{aligned} \tag{13}$$

Before the time $t = 0$, there is no circulation over the body. For ease of understanding, consider only 2 elements (panels), i.e., 2 lumped vortex elements and 2 collocation points are present at the quarter and three-fourths of the element, respectively. This implies that the influence coefficient matrix A is a square matrix of order 2.

Step-1: Calculate the influence coefficients A, B at collocation points (x_c, y_c) due to the presence of vortex element/wake element (as generated in further time steps) at (x_v, y_v).

Step-2: Find the unknown vortex strength and wake strength using the no-normal velocity boundary condition and Kelvin's circulation theorem.

At a time, say $t = t_1$, the circulations $\Gamma_{b_1}(t_1)$ and $\Gamma_{b_2}(t_1)$ develop at the quarter chord of each element and the first wake with strength $\Gamma_{w_1}(t_1)$ develops simultaneously as the timer starts from zero. The position of the upcoming wake is fixed at $0.1dx$ from the trailing edge of the flat plate, where dx is the length of the element. Thus, the unknowns at the first time step, i.e. at $t = t_1$ or time-index $m = 1$ are $\Gamma_{b_1}(t_1)$, $\Gamma_{b_2}(t_1)$ and Γ_{w_1}. These unknowns can be calculated using no normal velocity boundary condition (two collocation points, which give two equations) and the Kelvin circulation theorem (which gives one equation). As time progresses, the new wake gets generated at the same position as the earlier one, i.e., at $0.1dx$ from the trailing edge of the flat plate.

Now, consider the 3^{rd} time-step ($m = 3$), at which the unknowns will be $\Gamma_{b_1}(t_3)$, $\Gamma_{b_2}(t_3)$ and Γ_{w_3}. Thus, the induced normal velocities at each collocation point are given by:

$$\begin{bmatrix} v_{i1} \\ v_{i2} \end{bmatrix} = \begin{bmatrix} A_{11} & A_{12} \\ A_{21} & A_{22} \end{bmatrix} \begin{bmatrix} \Gamma_{b_1}(t_3) \\ \Gamma_{b_2}(t_3) \end{bmatrix} + \begin{bmatrix} B_{11} \\ B_{21} \end{bmatrix} \Gamma_{w_1} + \begin{bmatrix} B_{12} \\ B_{22} \end{bmatrix} \Gamma_{w_2} + \begin{bmatrix} B_{13} \\ B_{23} \end{bmatrix} \Gamma_{w_3} \quad (14)$$

The freestream velocity U_∞ will have a component in the normal direction (when converted to the body frame), given by $U_\infty \sin\alpha$, which depends on α. Also, since the plate is flapping, its motion will lead to a component of velocity, which is $-\dot{y}\cos\alpha$. Thus, the no-normal velocity boundary condition leads to:

$$\begin{bmatrix} A_{11} & A_{12} \\ A_{21} & A_{22} \end{bmatrix} \begin{bmatrix} \Gamma_{b_1}(t_3) \\ \Gamma_{b_2}(t_3) \end{bmatrix} + \begin{bmatrix} B_{11} \\ B_{21} \end{bmatrix} \Gamma_{w_1} + \begin{bmatrix} B_{12} \\ B_{22} \end{bmatrix} \Gamma_{w_2} + \begin{bmatrix} B_{13} \\ B_{23} \end{bmatrix} \Gamma_{w_3} + \begin{bmatrix} U_\infty \sin\alpha - \dot{y}\cos\alpha \\ U_\infty \sin\alpha - \dot{y}\cos\alpha \end{bmatrix} = 0 \quad (15)$$

Applying Kelvin's circulation theorem at 3^{rd} time-step:

$$\Gamma_{b_1}(t_3) + \Gamma_{b_2}(t_3) + \Gamma_{w_1} + \Gamma_{w_2} + \Gamma_{w_3} = 0 \quad (16)$$

Extending the above argument for 'N' collocation points and repacking all the equations in the matrix form, Eqn. 17 is obtained, and the strength of all body vortices and the strength of the wake generated at the m^{th} time step can be computed.

$$C \begin{bmatrix} \Gamma_{b_1}(t_m) \\ \Gamma_{b_2}(t_m) \\ \vdots \\ \Gamma_{b_N}(t_m) \\ \Gamma_{w_m} \end{bmatrix} = \begin{bmatrix} -EF - \sum_{j=1}^{m-1} B_{1j}\Gamma_{w_j} \\ -EF - \sum_{j=1}^{m-1} B_{2j}\Gamma_{w_j} \\ \vdots \\ -EF - \sum_{j=1}^{m-1} B_{Nj}\Gamma_{w_j} \\ -\sum_{j=1}^{m-1} \Gamma_{w_j} \end{bmatrix} \quad (17)$$

where,

$$C = \begin{bmatrix} A_{11} & \dots & A_{1N} & B_{1m} \\ A_{21} & \dots & A_{2N} & B_{2m} \\ \vdots & \ddots & \vdots & \vdots \\ A_{N1} & \dots & A_{NN} & B_{Nm} \\ 1 & \dots & 1 & 1 \end{bmatrix} \quad (18)$$

Moreover, $EF = U_\infty \sin\alpha - \dot{y}\cos\alpha$ is the external flow (EF) and common to all the terms in Eqn. 15. The reason behind the summation over the term in the RHS of Eqn. 17 $B_{ij}\Gamma_{w_j}$ running from $j = 1$ to $j = m-1$ is that, at the m^{th} time step, the wake strength and the influence coefficients at the collocation points due to the wakes generated at $(m-1)^{th}$ time step are known while that of the wake generated at m^{th} time step is yet to be calculated. Solving this system of linear equations (using LU decomposition), the strength of the body vortices and the new wake vortex is known.

Step-3: The next step is to calculate the induced velocities at the location of all the wakes due to all the body vortices and the other wake vortices.

Step-4: The position of all the wakes can then be updated using the formula:

$$\begin{aligned} x_w &= x_w + u_w dt \\ y_w &= y_w + v_w dt \end{aligned} \quad (19)$$

where, u_w and v_w are the induced velocity components computed in Step-3.

In the code, the matrix B is represented as a vector `B`, which is the last column B_{im} (the constant part). The rest of the matrix is computed directly with the computation of RHS of Eqn. 17. This is done for the ease of computation.

PARALLELIZATION STRATEGY

Many sections were identified in the code, which can be parallelized. These are:

1. Initializing the body vortex locations (`vorcloc`), collocation points (`colcloc`).
2. Initialization of A matrix and B vector.
3. Initialization of C matrix.
4. LU Decomposition of C matrix.
5. Computation of coordinates of origin and external flow EF at each instant.
6. Computation of RHS of Eqn. 17 (vector `R`).
7. Computation of induced velocities u_w and v_w.
8. Computation of lift and drag terms.

A common `#pragma omp parallel` region encapsulates the entire computation to avoid overheads of forking and joining the threads repeatedly. Certain sections, like forward and backward substitution to find the unknowns in Eqn. 17, have to be run serially. Such sections are run using a `#pragma omp single`, meaning whichever thread is free will serially run that section while others wait.

RESULTS

The code was tested for the following parameters:

1. Number of panels $N_l = 1000$
2. Number of time steps $N_t = 1001$
3. Free-stream velocity $U_\infty = 20$ m/s
4. Chord length $c = 10$ m
5. Angle of attack $\alpha = 0°$s

Figure 4 shows the wake structure generated by the serial code. Figure 5 does the same for parallel code.

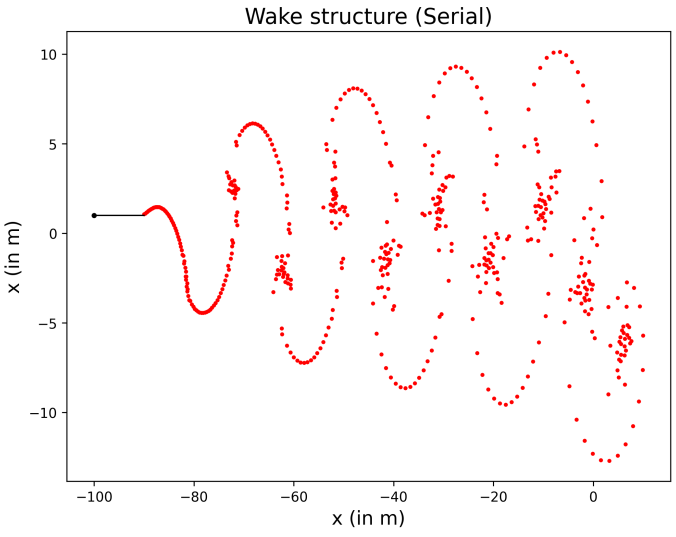

FIGURE 4. Wake structure from Serial code

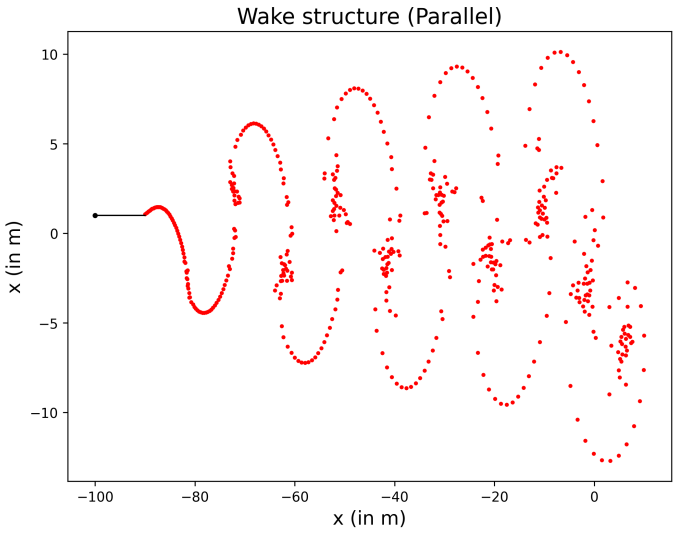

FIGURE 5. Wake structure from Parallel code

It can be seen that the structures are identical, which means that the parallel code is working correctly. For the given parameters, the serial run time was 123.6224 secs. The parallel runtimes are given in Tab. 1.

Number of threads p	Runtime (in s)
2	80.4538
4	69.8730
8	55.4219
16	59.8408

TABLE 1. Parallel runtimes for various processor count

Figure 6 plots the data in Tab. 1. It can be seen that the least time is for eight processors. Even for other processor counts, like for $p = 2$, the decrease in time is around 2/3rds instead of the expected 1/2. This shows that the amount of gain from parallelization is not that much.

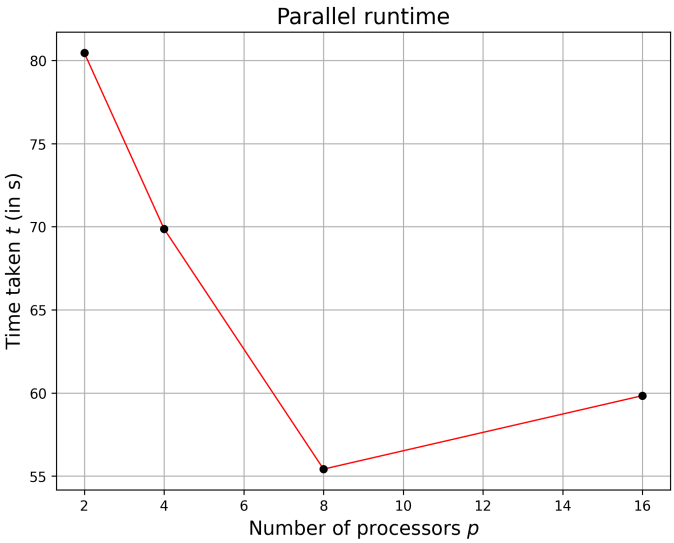

FIGURE 6. Parallel runtimes for various processor count

Figure 7 plots the parallel code's speed-up $\psi(n,p)$ for the different processor counts. This shows the same result as Fig. 6.

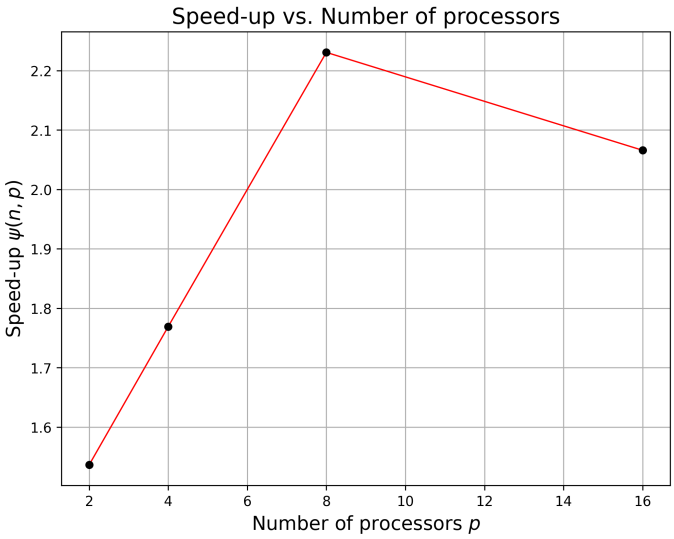

FIGURE 7. Speed-up for various processor count

Figure 8 plots the Karp-Flatt metric e of the parallel code for the different processor counts. This shows that until $p = 8$, there is scope for improvement in runtimes, which is also seen in the actual runtimes. However, after that, e starts to fall, meaning that the overheads associated with the parallelization dominate over the speed-up obtained. Thus, for this particular problem, the ideal processor count is 8. This also shows the limited parallelization possible in the problem.

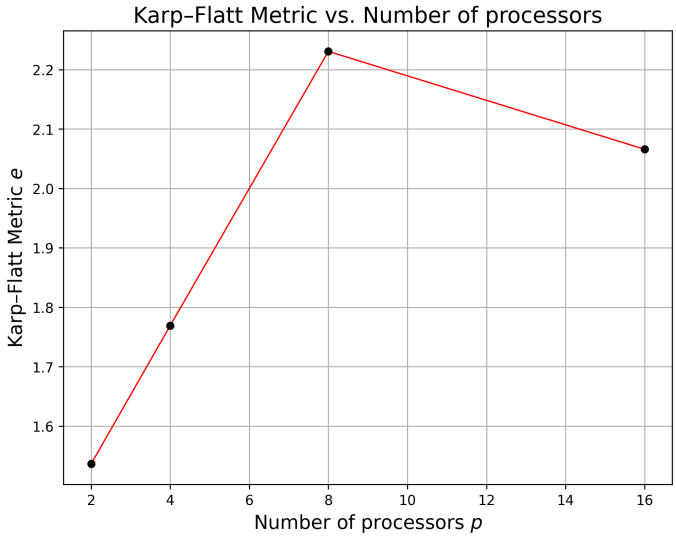

FIGURE 8. Karp-Flatt metric for various processor count

CONCLUSIONS

In this project, a serial code for simulating the wake structure behind a flapping flat plate was successfully parallelized using OpenMP. The results were compared to ensure that the parallel code was still giving the correct result. Then, the performance improvements obtained due to parallelization were studied by plotting parallel runtimes, speed-up obtained and the Karp-Flatt metric, all against the number of processors. It was concluded that the improvement was limited, and the time taken had started to increase beyond eight threads. The most probable reason is the increased overheads associated with the parallelization overcoming the improvement obtained.

ACKNOWLEDGMENT

Thanks to Prof. Kameswararao for teaching this course excellently and guiding us throughout the course whenever we had any doubts.

REFERENCES

[1] Katz, J., and Plotkin, A., 2001. *Low-Speed Aerodynamics*. Cambridge Aerospace Series. Cambridge University Press.